HHS Public Access

Author manuscript

Adv Nanobiomed Res. Author manuscript; available in PMC 2024 February 01.

Published in final edited form as:

Adv Nanobiomed Res. 2023 February ; 3(2): . doi:10.1002/anbr.202200130.

Outer Membrane Vesicle-Coated Nanoparticle Vaccine Protects Against *Acinetobacter baumannii* Pneumonia and Sepsis

Elisabet Bjanes[1], **Jiarong Zhou**[2], **Tariq Qayum**[1], **Nishta Krishnan**[2], **Raymond H. Zurich**[1], **Nitasha D. Menon**[1,3], **Alexandria Hoffman**[1], **Ronnie H. Fang**[2], **Liangfang Zhang**[2,*], **Victor Nizet**[1,4,*]

[1]Division of Host-Microbe Systems and Therapeutics, Department of Pediatrics, University of California San Diego, La Jolla, California 92093, USA

[2]Department of Nanoengineering, University of California San Diego, La Jolla, California 92093, USA

[3]School of Biotechnology, Amrita Vishwa Vidyapeetham, Amritapuri, Kerala, India

[4]Skaggs School of Pharmacy and Pharmaceutical Sciences, University of California San Diego, La Jolla, California 92093, USA

Abstract

The highly multidrug-resistant (MDR) Gram-negative bacterial pathogen *Acinetobacter baumannii* is a top global health priority where an effective vaccine could protect susceptible populations and limit resistance acquisition. Outer membrane vesicles (OMVs) shed from Gram-negative bacteria are enriched with virulence factors and membrane lipids but heterogeneous in size and cargo. We report a vaccine platform combining precise and replicable nanoparticle technology with immunogenic *A. baumannii* OMVs (Ab-OMVs). Gold nanoparticle cores coated with Ab-OMVs (Ab-NPs) induced robust IgG titers in rabbits that enhanced human neutrophil opsonophagocytic killing and passively protected against lethal *A. baumannii* sepsis in mice. Active Ab-NP immunization in mice protected against sepsis and pneumonia, accompanied by B cell recruitment to draining lymph nodes, activation of dendritic cell markers, improved splenic neutrophil responses, and mitigation of proinflammatory cytokine storm. Nanoparticles are an efficient and efficacious platform for OMV vaccine delivery against *A. baumannii* and perhaps other high-priority MDR pathogens.

Table of Contents

Novel vaccines effective against multidrug resistant bacteria, including *Acinetobacter baumannii*, are a major priority for global health. Outer membrane vesicles (OMVs) shed from bacterial membranes are highly immunostimulatory, but heterogenous. We designed a vaccine that

[*]**Corresponding author:** zhang@ucsd.edu (L.Z.) or vnizet@ucsd.edu (V.N.).

Author Contributions

V.N., L.Z., E.B., J.Z., and R.H.F. conceived the idea and designed the experiments. E.B., J.Z., T.Q., N.K., R.H.Z., N.D.M., and A.H. performed all experiments. All authors analyzed and discussed the data. E.B., J.Z., R.H.F., L.Z. and V.N. wrote the paper.

The authors declare no competing financial interest.

Supporting Information

Supporting Information is available from the Wiley Online Library or from the author.

combines precision nanotechnology with OMVs from *A. baumannii* (Ab-NPs). Active Ab-NP immunization in mice protected against sepsis and pneumonia, accompanied by B cell recruitment to draining lymph nodes, activation of dendritic cell markers, improved splenic neutrophil responses, and reduction of proinflammatory cytokine activation.

Keywords

nanoparticle vaccine; outer membrane vesicle; multidrug-resistant bacterial infection; *Acinetobacter baumannii* ; pneumonia; sepsis

1. INTRODUCTION

Antimicrobial resistance (AMR) is an exigent threat to global public health, with recent statistical estimates of 4.95 million deaths associated with, and 1.27 million directly attributable to, multidrug-resistant (MDR) bacterial infections worldwide in 2019.[1] As successful development of new antibiotics has dwindled in recent decades, vaccine technologies have continued to advance.[2,3] Thus, prevention of infections by emerging MDR pathogens through novel vaccine development has gained support as a critical element of the battle against AMR.[4–6] The application of innovative nanotechnologies in vaccine formulation has increased sharply in recent years, offering advantages of improved stability, protection from premature degradation, and precise delivery to desired cellular targets.[7–9] The tunability of nanoparticles to precise sizes for maximal immunogenicity and uptake by antigen presenting cells is a particularly important facet of these lines of translational research.[7]

Outer membrane vesicles (OMVs) are naturally occurring, non-replicating, highly immunogenic, spherical nanostructures that are shed from the surface of Gram-negative bacteria.[10–12] The diverse biological functions of OMVs include horizontal gene transfer,[13] delivering microRNAs[14] and virulence factors[15,16] into host cells, immune evasion by inactivating host defense factors,[17,18] resistance to antibiotics,[19] nutrient acquisition,[20] quorum sensing,[21] and stress responses.[22] Because they display an array of bacterial surface proteins, lipids and carbohydrates, as well as cell wall components with adjuvant properties, several strategies have explored OMVs as an alternative to whole cell bacterial vaccines;[10–12,23,24] indeed OMVs from *Neisseria meningitidis* serogroup B are included along with bacterial proteins from the pathogen in a multicomponent vaccine (Bexsero®) that is approved for human use.[25] Nevertheless, the development of OMVs as a vaccine or drug product poses certain complexities, in particular related to heterogeneity in size,[26] yield, potential differences in the internal cargo they carry, and their structural stability in face of various physical or chemical stresses.[27]

In this study, we explore whether a nanotechnology based on citrate-stabilized gold nanoparticles (AuNPs) could be used to enhance the consistency and stability of an OMV-based bacterial vaccine while maintaining optimal immunogenicity. For these proof-of-principle studies, we selected the frequently MDR opportunistic Gram-negative bacterial pathogen *Acinetobacter baumannii*, which is named an urgent threat by the U.S. Centers for Disease Control and Prevention[28] and sits atop the World Health Organization

global priority pathogens list of antibiotic-resistant bacteria.[29] Nosocomial *A. baumannii* infections such as hospital- or ventilator-acquired pneumonia (HAP/VAP), sepsis, urinary tract infections, and wound infections[30] have associated mortality rates between 25–80%, depending on infection type and location.[31,32] MDR prevalence among *A. baumannii* strains is extremely high at 80%, with >50% of isolates on most continents resistant to carbapenems, an antibiotic class of last resort.[32] *A. baumannii* infects medically vulnerable populations—risk factors include mechanical ventilation, prolonged antimicrobial or immunosuppressive therapy, comorbidities such as diabetes and chronic lung disease, severe trauma or burns, and most recently, COVID-19 pneumonitis.[33–35]

A vaccine against endemic *A. baumannii* could provide essential protection to vulnerable populations without further exacerbating antibiotic resistance.[32,36,37] Although such vaccine candidates have been tested in rodents, none have progressed past pre-clinical investigations.[36] With respect to *A. baumannii* OMVs (Ab-OMVs), their secretion is dependent on outer membrane protein A (OmpA), which is subsequently highly enriched on the Ab-OMV surface. OmpA facilitates delivery of *A. baumannii* virulence factors into the host cell cytoplasm.[38] Since Ab-OMVs are coated with OmpA, virulence factors, and membrane lipids, they are strongly immunogenic;[39] however, their heterogeneity and variable cargo poses a challenge for large-scale clinical testing and manufacturing.[30,40]

Here we apply cell membrane coating technology to functionalize AuNPs with Ab-OMVs and engineered a tunable *A. baumannii* nanoparticle vaccine (Ab-NP).[41] Use of a nanoparticle core enabled us to fine tune nanovaccine size for efficient lymphatic transport and immune processing, otherwise hard to achieve with pure OMV-based formulations.[42,43] We found that Ab-NP vaccination induced robust IgG antibody responses in both rabbits and mice, and that the antisera promoted opsonophagocytic killing (OPK) of *A. baumannii* by human neutrophils. Ab-NP vaccination induced superior B cell recruitment to the draining lymph nodes and increased dendritic cell activation compared to Ab-OMV only and PBS controls. Most importantly, passive immunization with immune serum and active Ab-NP vaccination strongly protected mice against lethal sepsis and pneumonia in challenge studies with a hypervirulent *A. baumannii* strain. Combining immunogenic OMVs with nanotechnology thus merits further exploration as a platform for vaccine development against *A. baumannii* and other MDR Gram-negative bacterial pathogens.

2. RESULTS

To engineer Ab-OMV bound nanoparticles (Ab-NPs), we coated 30 nm citrate-stabilized gold particles (AuNPs) with OMVs isolated and purified from the hypervirulent, clinical outbreak-associated *A. baumannii* strain Lac-4[44] by an established protocol (Figure 1, see Methods for details).[42,45,46] AuNPs have been utilized in nanotechnology for decades and were chosen as the core for this novel application due to their reliability, ease of synthesis, and superior uptake by immune cells.[47] The small size of AuNPs also allows for efficient lymphatic drainage into secondary lymphoid organs for antigen presentation and processing.[43]

An inherent property of uncoated AuNPs is their tendency to rapidly aggregate in PBS, which can be visualized by a change in color (Figure 2A). Optimal membrane coating was determined by evaluating the stability of Ab-NPs fabricated at various Ab-OMV to AuNP ratios (Figure S1). At a 1:1 weight ratio, the resulting Ab-NPs were stable upon transfer to PBS, and this ratio was utilized in subsequent experiments. A sharp drop in membrane protein loading efficiency beyond the 1:1 ratio indicated a saturation in the membrane coating (Figure 2B). For the optimized Ab-NP formulation, protein loading was 88.6 ± 0.45 μg Ab-OMVs per mg of AuNPs with a loading yield of 8.14 ± 0.04%; considering the high density of gold, excellent coverage of the AuNPs by the bacterial membrane was achieved. Consistent with OMVs from other Gram-negative bacteria,[26] dynamic light scattering (DLS) measurements revealed high heterogeneity in size distribution of Ab-OMVs, with diameters ranging from 30–5000 nm (Figure 2C and 2D).[48,49] In contrast, AuNPs were uniformly distributed with a hydrodynamic size of 34.18 ± 1.63 nm and a slight shift in size to 45.54 ± 0.27 nm after coating, consistent with the addition of a several nm thick membrane layer. Successful coating was further verified by zeta potential measurements where the value of uncoated AuNPs increased after coating to a value statistically similar to Ab-OMVs (Figure 2E). Coated Ab-NPs maintained remarkably consistent size distribution even after 7 days due to the stability provided by the OMV layer (Figure 2F). Ab-OMV association with AuNPs and the completeness of the membrane coating were visually confirmed by transmission electron microscopy (TEM), where spherical AuNP cores were found wrapped with an additional thin layer of membrane (Figure 2G). In contrast, visualization of Ab-OMVs showed heterogenous vesicles of varying sizes (Figure 2H). Coomassie blue dye staining of *A. baumannii* Lac-4 lysate, Ab-OMVs, uncoated AuNPs, and Ab-NPs confirmed protein banding patterns in the coated Ab-NPs comparable to OMVs (Figure 2I). Importantly, Ab-NPs were not cytotoxic to murine bone-marrow derived dendritic cells (BMDCs) at concentrations up to 10 μg/mL (Figure 2J). Together these biophysical studies document the uniformity and preliminary safety profile of the Ab-NP vaccine candidate.

To test whether Ab-NPs could generate a protective antibody response, we obtained immune rabbit serum by vaccinating two New Zealand white rabbits with 1 mg of Ab-NPs without additional adjuvants. Compared to pre-vaccination (pre-vax) serum controls, post-vax rabbit serum had significantly increased immunoglobulin G (IgG) titers (~2.5 $\log_{10}$ fold, Figure 3A) and enhanced binding intensity and percent IgG binding (Figure 3B–3D) to logarithmic-phase *A. baumannii*, respectively in a neutralization assay. Furthermore, opsonization with post-vax serum improved *A. baumannii* killing by healthy human neutrophils by 100-fold compared to pre-vax serum (Figure 3E).

To assess the protective capacity of the post-vax serum *in vivo*, we established an intraperitoneal (IP) sepsis model with the *A. baumannii* Lac-4 strain.[50] Mice rapidly succumb to infection in a dose-dependent fashion with an LD_{80} of 10^6 colony forming units (CFU) of the bacterium (Figure 3F). Hypothermia is a hallmark of experimental Gram-negative sepsis, and *A. baumannii* induced an acute dose-dependent temperature drop in the mice within 6 h of bacterial challenge (Figure 3G). For passive immunization studies, mice received either post-vax or naive rabbit serum intravenously at days −2 and 0 (Figure 3H), with successful antibody transfer confirmed by submandibular cheek bleeding

and ELISA—namely an ~2.5-$\log_{10}$-fold increase in anti-*A. baumannii* IgG titer in animals receiving post-vax serum compared to naive serum (Figure 3I). Two days following passive immunization, mice were challenged IP with *A. baumannii* Lac-4. All animals that received two doses of post-vax serum survived the infection compared to 20% and 100% mortality among the single dose post-vax and naïve serum cohorts, respectively (Figure 3J). Passive antibody transfer also protected mice from sepsis-induced hypothermia (Figure 3K). These results confirm that immune serum generated from Ab-NP vaccination specifically binds to *A. baumannii* and protects against lethal sepsis in mice.

Encouraged by the passive immunization findings, we next investigated recruitment and activation of antigen presenting cells (APCs) to the draining lymph nodes. We vaccinated mice subcutaneously in the flank with mock control, Ab-OMVs or Ab-NPs. Twenty-four hours post-vaccination, inguinal lymph nodes were harvested and processed for single cell isolation, staining, and flow cytometric analysis. Ab-NP vaccination induced significantly higher percentages of B cells relative to mock or Ab-OMVs (Figure 4B) and increased expression of the activation markers CD40, CD80, CD86, and MHCII on $CD11c^+$ dendritic cells (Figure 4C, 4D, and S2). Thus the Ab-NP vaccine induced robust B cell recruitment and DC activation to the draining lymph node, consistent with prior reports of improved APC activation by nanoparticle vaccines relative to OMV only controls.[51–53] Ultimately, a major consideration of clinical product manufacturing is reducing batch variability and improving product reliability and homogeneity. Our initial studies find improved homogeneity of Ab-NPs relative to Ab-OMVs (Fig 2B) and similar or enhanced APC responses (Fig 4B). We therefore proceeded to test the safety and efficacy of Ab-NP vaccination in murine models.

We next examined the antigenicity and murine safety profile of Ab-NP vaccination. Mice were vaccinated with three successive doses of Ab-NPs, red blood cell-coated NPs (RBC-NPs) or mock as vehicle controls (Figure 5A). Mice were cheek-bled weekly to assess IgG titer. Mice immunized with Ab-NP generated a robust IgG antibody response specific for *A. baumannii* that was ~4 $\log_{10}$-fold higher than RBC-NP and mock controls (Figure 5B). In vaccine safety assessment, animal body weight change is a key baseline metric.[54,55] No significant weight changes were seen in mice that received Ab-NP vaccination vs. RBC-NP or mock control (Figure S3A and S3B). Likewise, toxicity of Ab-NP vaccination to the hematopoietic compartment was not observed, as white blood cell (WBC) count increased only 1.5 fold on day 3 compared day −1 prior to immunization; less than a 10-fold change is considered safe[54,55] (Figure S3C and S3D,). Moreover, no leukopenic toxicity was seen for Ab-NP relative to RBC-NP (Figure S3E, cyclophosphamide used as positive control). To exclude potential impacts on kidney function, we analyzed serum creatinine 24 h after the first vaccination dose for an acute measurement and 24 h post the third dose for delayed toxicity (Figure S3F). No increases in serum creatinine levels were seen in mice after Ab-NP vaccination, indicating kidney function was not impaired. We further examined two markers for liver function, serum aspartate aminotransferase (AST) and alanine aminotransferase (ALT) and found no changes from baseline for either enzyme after Ab-NP vaccination (Figure S3G and S3H). These initial analyses are encouraging that Ab-NP vaccination is safe in the murine preclinical model.

Knowing our vaccine can generate a specific antibody response and is tolerated by mice, we next investigated the efficacy of protection. Mice were vaccinated with three doses of RBC-NPs, Ab-OMVs, or Ab-NPs. Two weeks after the third dose, mice were challenged intraperitoneally with Ab Lac-4 in a disseminated sepsis model. Immunized mice were completely protected against lethal septic challenge with the hypervirulent *A. baumannii* strain (Figure 5C, S4). To establish the duration of protection generated by Ab-NP vaccination, we vaccinated mice with RBC-NPs or Ab-NPs and monitored titers for six months. Although anti-Ab Lac-4 titers declined modestly between 12–26 weeks, Ab-NP vaccination still protected 90% of mice from a lethal sepsis infection without additional booster doses (Figure S3I and S3J). Thus, we find our three-dose regimen is highly efficacious at protecting mice from lethal *A. baumannii* infection for a period of at least six months. To determine whether protection in immunized mice correlated with lower bacterial burdens, we first established that *A. baumannii* Lac-4 rapidly disseminates to systemic organs 4 h after IP infection in a dose-dependent manner (Figure 5D). In separate cohorts of mice, we found that Ab-NP immunization markedly accelerated bacterial clearance, with a 3 to 5 $\log_{10}$-fold reduction in *A. baumannii* CFUs in organs (spleen, liver and kidney) and undetectable CFU in the blood (Figure 5E).

Gram-negative sepsis is characteristically accompanied by an overwhelming cytokine storm —thus we investigated whether Ab-NP vaccination could contain uncontrolled release of inflammatory mediators following infection. Notably, Ab-NP vaccination dampened systemic inflammation as measured by significant decreases in serum IL-6, IL-1β, and TNF-α levels (Figure 5F–5H). Neutrophils are an essential immune responder during *A. baumannii* infections,[56,57] and neutropenia is a significant risk factor for bacteremia and associated mortality.[58,59] To assess Ab-NP vaccine effects on neutrophil responses in the mouse model, we harvested and processed spleens 4 h post-infection for single cell isolation, staining, and analysis by flow cytometry. Ab-NP vaccinated mice had significantly more splenic neutrophils, both in percentage and total numbers, relative to RBC-NP and mock treated mice (Figure 5I–5K). These data suggest Ab-NP vaccination boosts the recruitment of neutrophils to the spleen upon Ab-NP trapping and/or increases neutrophil survival during the direct host-pathogen encounter.

A. baumannii is a leading cause of hospital- and ventilator-acquired pneumonia.[30] In a murine intratracheal challenge model of pneumonia (Figure 6A), we found that the hypervirulent *A. baumannii* Lac-4 strain produced similar mortality rates at a 10-fold lower challenge dose than the commonly studied AB5075 strain[60] (Figure 6B). To assess the protective effect of Ab-NP vaccination in this model, mice were immunized with mock, RBC-NPs or Ab-NP and bled weekly for IgG antibody titers. Four weeks post initial vaccination, mice were challenged intratracheally with *A. baumannii* Lac-4. Consistent with our findings in the sepsis model, Ab-NP immunized mice, which had significantly higher titers than the control mice, were completely protected from pneumonia-induced mortality (Figure 6C and 6D). Lastly, we assessed the long-term protective capacity of Ab-NP vaccination in a pneumonia model by vaccinating mice with RBC-NPs or Ab-NPs. Mice were challenged intratracheally 30 weeks post-vaccination with Ab Lac-4 and monitored daily. We saw Ab-NP vaccination provided 100% protection even after 7 months with no

additional boosters (Figure 6E), consistent with our findings that vaccination also protects long-term against disseminated sepsis (Figure 4G).

3. DISCUSSION

A. baumannii is an increasingly important cause of nosocomial pneumonia and sepsis for which treatment and environmental eradication are exceptionally difficult.[61–63] We have developed an *A. baumannii* OMV-based, nanoparticle-stabilized vaccine prototype that protects mice from lethal sepsis and pneumonia. Ab-NP vaccination induces a robust IgG antibody response specific to *A. baumannii* that promotes human neutrophil opsonophagocytic killing and confers protection against sepsis on passive transfer. Active immunization with Ab-NP protected against lethal *A. baumannii* sepsis with rapid reduction of bacterial counts in blood and organs and likewise provided protection against the pathogen in a pneumonia model. Ab-NP vaccination stimulates superior B cell recruitment to inguinal lymph nodes and increased DC activation and maturation relative to PBS and Ab-OMV controls, and further promoted the survival and recruitment to the spleen of neutrophils that are essential in innate defense against *A. baumannii*.

The extreme prevalence of MDR[64] and remarkable ability to acquire novel resistance among circulating *A. baumannii* strains prompts an urgent need for non-antibiotic solutions. While multiple vaccine candidates have been tested against *A. baumannii*, none have progressed to clinical studies.[32] Successful vaccine candidates against other Gram-negative bacteria have utilized OMVs, the non-replicative, cargo-containing vesicles released by *A. baumannii* Gram-negative species.[26,65] Ab-OMVs potential as vaccine antigens lies in the immunogenicity of their membrane antigens, ability to potentiate uptake by immune cells, and stimulatory contents.[26,65] Despite these advantages, OMVs exhibit high heterogeneity in size distribution, which could influence their uptake by antigen presenting cells. Macrophages prefer larger particles (0.5–5 μm) while dendritic cells preferentially ingest smaller debris (0.04–0.1 μm).[66] Furthermore, antigen size significantly instructs the immune response, with particles between 40–50 nm inducing increased CD8 and CD4 Th1 responses relative to particles >0.5 μm.[67]

When designing our vaccine, we considered manufacturing concerns as well as efficacy and safety. Paramount to Good Manufacturing Practices (GMP) regulations promulgated by the U.S. FDA are quality control practices that ensure safe, efficacious, and highly reliable products. While OMVs are strongly immunostimulatory, their heterogeneity results in batch variability that could render large scale manufacturing impractical or cost prohibitive, whereas the defined nature of the Ab-NP formulation could help to overcome these challenges. AuNPs have been utilized for decades in biological research and have a proven record of reliable and tunable fabrication.[68] We investigated whether combining OMVs with nanotechnology could serve as a safe and consistent platform for vaccine delivery.

We engineered a unique nanoparticle vaccine against *A. baumannii* by coating AuNPs with OMVs released by a hypervirulent clinical isolate of the pathogen (Lac-4). The Ab-NP vaccine is highly immunostimulatory and protective in both sepsis and pneumonia models in mice even up to six months after vaccination. Consistent with our targeted antigen size, Ab-

NP vaccination induced significant B cell recruitment and DC maturation in draining lymph nodes that exceeded immunization with Ab-OMVs alone. Robust IgG antibody responses specific to *A. baumannii* after vaccination protected in active and passive immunization and potentiated the killing capacity of healthy human neutrophils, supporting our hypothesis that the combination of nanoparticle technology and OMV immunogenicity is an effective approach for vaccine design. While we elected to employ AuNPs in our study due to proven consistency and utility in fabrication, other nanomaterials such as polymeric or iron oxide nanoparticles can similarly act as the stabilizing core.[41] The choice of core material can bestow additional functionalities, such as inclusion of additional adjuvants or magnetic guidance, although these additions were not necessary in our current Ab-NP formulation.

One potential hurdle that has previously arisen with OMV vaccines is the presence of lipopolysaccharide (LPS), a major component of Gram-negative cell membranes.[69] Humans are approximately 1000 times more sensitive to LPS than mice, which can lead to serious side effects such as endotoxic shock.[70] Interestingly, *A. baumannii* is one of three Gram-negative bacteria that is capable of surviving loss of the immunostimulatory lipid A component of LPS.[30] Unlike LPS-deficient *Neisseria meningitis* and *Moraxella catarrhalis* that were both constructed *in vitro,*[71,72] recent studies have found that naturally occurring *A. baumannii* clinical isolates modify LPS synthesis genes to escape host immunity and antibiotic pressure.[73] While these strains are less immunostimulatory *in vitro,*[74] their presence in the clinical disease suggests that LPS deficiency does not entail the same fitness or virulence deficit observed with LPS-deficient *N. meningitidis* and *M. catarrhalis.*[71,72] A previous study found that adjuvanted Ab-OMVs derived from an LPS-deficient strain of *A. baumannii* provided 75% protection in a lethal sepsis model.[75] If the presence of LPS in Ab-NP proved concerning for toxicity or safety issues, substitution of LPS-minus Ab-OMVs into the nanoparticle platform could be achieved.

Until recently, murine sepsis models had been limited to extremely high inoculums and immunocompromised mice,[50,76] but our studies employed the clinical isolate Lac-4 that is acutely lethal in healthy mice at much lower doses than other commonly utilized *A. baumannii* strains. However, *A. baumannii* frequently infects individuals whose immune systems are impaired through injury, trauma, disease, or immunosuppression. We thus plan future studies to examine the efficacy of Ab-NP in specialized experimental mouse models of chemotherapy-induced neutropenia, diabetes, pregnancy, or major surgery. Future directions of this work also include expanding the repertoire of *A. baumannii* strains used to prepare the OMVs, since although OmpA has >90% conservation across strains,[77] outer membrane and capsule heterogeneity are likely to result in variable cross-strain protection from a single OMV-derived vaccine.[78]

In summary, we have found Ab-NP to be an effective and novel nanoengineered vaccine candidate that is highly protective against *A. baumannii* sepsis and pneumonia. Our work provides proof-of-principle that OMV-coated NPs can serve as a consistent and tunable platform for rapid vaccine production and testing for high priority MDR Gram-negative pathogens.

4. METHODS

Experimental Design.

The objective of this study was to design and validate an OMV-coated nanoparticle vaccine that protects against lethal sepsis and pneumonia caused by a hypervirulent clinical isolate of *A. baumannii*.

Bacterial Strains and Culture.

A. baumannii Lac-4 is an outbreak strain isolated from an LA county hospital in 1997[44] and obtained from Wangxue Chen (National Research Council, Canada).[76] The strain was grown in tryptic soy broth (TSB) with aeration at 37°C. Stationary phase overnight cultures were sub-cultured in TSB and grown to mid-logarithmic phase with aeration at 37°C and washed with PBS prior to use in experiments. Strain AB5075 was isolated from a patient with tibial osteomyelitis[60] and acquired from the Walter Reed Medical Center and was handled as above substituting the similar growth medium cation-adjusted Mueller Hinton Broth (Ca-MHB).

Ab-OMV Derivation.

Single colonies of *A. baumannii* Lac-4 were inoculated in 1.5 L flasks of TSB and grown for 16 h at 37°C with aeration. Stationary-phase cultures were spun down in a Sorvall RC-6 refrigerated floor centrifuge for 10 min at 10,000 rpm. The supernatant was filtered through a 0.45 μm PES vacuum filter (Thermo Fisher, 167-0045) and concentrated nearly 100 times by tangential flow filtration. Ab-OMVs were spun down by ultracentrifugation at 150,000 *g* for 2 h at 4°C, resuspended with water, and stored in −80 °C.

Ab-NP Production.

Citrate stabilized 30-nm AuNPs (NanoComposix, AUCN30) were mixed with Ab-OMVs at different weight to protein ratios and sonicated in a bath sonicator for 2 min for coating. The mixture was then washed once with water by centrifugation at 5,000 *g* for 15 min to remove any free Ab-OMVs and used immediately. Preparation of RBC-NP controls were fabricated in a similar fashion with murine RBC membrane.

Ab-NP Characterization.

Protein loading was determined using a bicinchoninic acid assay kit (Thermo Fisher, 23227), and size, polydispersity index, and zeta potential were measured by dynamic light scattering. OMV loading efficiency was defined by the percent of OMVs bound to AuNPs compared to the input OMVs. Stability was tested by adjusting Ab-NP to 1×PBS and storing the sample at 4°C for a week. To image the nanoparticles under TEM, samples were concentrated down to 0.5 mg/mL and 5 μL was deposited onto a TEM grid. The sample was dried and then negatively stained with 1% uranyl acetate for visualization. To confirm proper protein transfer, all samples were normalized to a protein concentration of 0.25 mg/mL, diluted with lithium dodecyl sulfate loading buffer (Thermo Fisher, NP0007), and run at 165 V for 45 min in MOPS running buffer (Thermo Fisher, B0001) for separation. The separated proteins were visualized by staining the gel with InstantBlue (Abcam, ISB1L) for 1 h followed

by overnight washing with water. BMDC viability was evaluated by incubating varying concentrations of Ab-NP with 25,000 BMDC in 96-well plates for 3 days at 37°C, 5% CO_2. Viability was evaluated using PrestoBlue according to the manufacturer's instructions.

Immunized Rabbit Sera.

Two New Zealand White rabbits were immunized with four successive doses of 0.25 mg Ab-NP subcutaneously with each dose two weeks apart at AbCore (Ramona, CA). Rabbits were bled before (pre-vax) and after vaccination (post-vax) and serum was isolated.

Murine and Rabbit IgG Neutralization Assays.

For ELISA assay, low-binding Immulon 4 HBX 96-well plates (Thermo Fisher, 3855) were coated with 1×10^8 CFUs/well of heat-killed *A. baumannii* Lac-4 in sodium bicarbonate buffer (Sigma, C3041). Coated plates were incubated overnight at 4°C, washed 3 times with PBST and blocked with 1% Reagent Diluent #2 (R&D Systems, DY995) for 1 h at room temperature or overnight at 4°C. Isolated rabbit or mouse serum was serially diluted in 1% Reagent Diluent #2 and incubated overnight at 4°C. Plates were washed three times with PBST and detected with goat anti-mouse (1:4000) or anti-rabbit (1:4000) IgG HRP (Southern Biotech, 1030-05 & 4030-05) in 1% Reagent Diluent #2 for 90 minutes at room temperature. Plates were washed 3x with PBST and incubated with streptavidin (R&D Systems, DY998) in 1% Reagent Diluent #2 for 30 min. Plates were washed three times with PBST and detected with TMB (BD, 555214) according to the manufacturer's instructions. Detection was halted with 2N H_2SO_4, and plates read on a spectrometer at 450 nm. Titers were determined using four-parameter logistics curve fit (Prism). For flow cytometry analysis, mid-logarithmic phase *A. baumannii* Lac-4 was blocked in 10% heat-inactivated horse serum (Sigma, H1138) at room temperature. 2% rabbit serum was subsequently incubated at room temperature in triplicate. Bacteria were washed and stained with goat anti-rabbit IgG AlexaFluor488 (Thermo Fisher, A-11008). Samples were washed and run on a BD FACS Canto II. Gates were drawn using single-stained pre-vax and unstained controls.

Renal and Liver Toxicity Screens.

Mice were vaccinated with 1 μg RBC-NPs, Ab-OMVs, or Ab-NPs on days 0, 7, and 14. Blood was collected from the submandibular vein, and serum was isolated on days 0 (before vaccination), 1, and 15. Serum creatinine was assessed using a creatinine (serum) colorimetric assay kit according to the manufacturer's instructions (Cayman Chemical, 700460). Serum AST and ALT were determined using ALT and AST colorimetric activity assay kits, respectively (Cayman Chemical, 701640, 700260).

Opsonophagocytic Killing Assays.

Blood from healthy human donors was collected by venipuncture into BD Vacutainer Plasma Tubes spray coated with sodium heparin (BD, 367874). Human neutrophils were isolated from healthy human donors with consent under protocols approved by the UCSD Institutional Review Board (Protocol #131002) as previously described.[79] Briefly, heparinized blood was layered onto PolymorphPrep (Cosmo Bio, NC0863559) and spun at

630 × *g* for 30 min. Neutrophils were isolated from the appropriate layer and washed with PBS. Following RBC lysis, neutrophils were counted by trypan blue exclusion and used immediately. *A. baumannii* strains were incubated with 20% pre-vax or post-vax rabbit sera for 30 min at 37°C. Serum coated bacteria were incubated with isolated healthy human neutrophils in triplicate at a multiplicity of infection (MOI) = 1 bacterial/cell for 2 h at 37°C, 5% CO_2. Neutrophils were lysed in dH2O for 3 min, serially diluted in PBS, and plated on tryptic soy agar (Sigma, 22092) for enumeration.

Murine Studies.

All animal studies were conducted in compliance with federal regulations listed in the Animal Welfare Act and based on the recommendations of the guide for the care and use of laboratory animals and the University of California San Diego Institutional Animal Care and Use Committee (IACUC). All protocols used in this study were approved by the IACUC at UCSD (Protocol #S00227M). Mice were housed in a specific pathogen free (SPF) facility on a 12 h light/dark cycle in pre-bedded corn cob disposable cages (Innovive). Mice were fed a 2020X diet (Envigo) and received acidified water. UCSD vivarium staff randomized mice 48–72 h prior to experimentation into cages with no more than 5 mice per cage. All experiments were conducted under the supervision of veterinarians.

Infection Models.

For the sepsis model, 8 to 12-week-old male and female C57BL/6J mice (Jackson Laboratory, 00664) were infected with 10^5, 10^6, or 10^7 CFUs log-phase *Acinetobacter baumannii* Lac-4 in sterile PBS intraperitoneally to induce disseminated sepsis. Surface body temperatures were monitored by infrared thermometry every 6 h for 24 h post-infection. Mice were monitored twice daily for survival for 7 days. For bacterial load determination, mice were humanely euthanized with CO_2 and confirmed by cervical dislocation according to IACUC approved protocols 4 h post infection. The spleen, liver, and kidneys were collected for CFU counts. Organs were disrupted with a MagNA Lyser (Roche) for 60 sec at 6000 RPM. Peritoneal CFUs were assessed with 10 mL PBS peritoneal lavage. Blood was obtained by cardiac puncture, serum was isolated and systemic cytokine levels (IL-6, IL-1β, and TNF-α) were assessed by ELISA. Spleens were processed for single cell isolation and stained for innate immune cell markers. PMNs were gated cells, singlets, live, CD11b+, $Ly6C^{int}/Ly6G^{hi}$. Gates were drawn using single-stained controls and fluorescence minus ones (FMOs). In the pneumonia model, Mice were infected with 10^6, 10^7, or 10^8 CFUs log-phase A. *baumannii* Lac-4 or 10^8 CFUs log-phase AB5075 in sterile PBS intratracheally. Mice were anesthetized with 100 mg/mL ketamine and 10 mg/mL xylazine prior to infection. Mice were monitored on a heating pad until fully recovered and monitored twice daily for 7 days.

Serum Cytokines.

Mice were humanely euthanized 4 hours post infection and blood obtained by cardiac puncture. Serum was isolated with serum separator tubes (BD, 365967) was isolated and systemic IL-6 (R&D Systems, DY406), IL-1β (R&D Systems, DY401), and TNF-α (R&D Systems, DY410) were assessed by ELISA according to the manufacturer's instructions.

Passive Immunization.

8 to 12-week-old female C57BL/6 mice were immunized intravenously through retro-orbital injection with 200 μL of naïve rabbit serum (Sigma, R4505) or 200 μL immune rabbit serum from immunized AbCore rabbits. One group of mice received a second dose of immune rabbit serum 24 h after the initial dose. Mice were briefly anesthetized with isoflurane prior to injection. Pre-vax and post-vax IgG titers were determined by submandibular cheek bleeding on Days −2 and 0 and by ELISA. Mice were challenged with 10^7 CFUs Ab Lac-4 IP on Day 0 and monitored every 6 h for body temperature for 24 h and twice daily for survival for 7 days.

Nanoparticle Vaccination.

4 to 5-week-old female C57BL/6 mice were immunized intraperitoneally with 1 μg Ab-NP, Ab-OMVs, or RBC-NPs in 100 μL PBS on Day 0, 7, and 14. Mock mice were immunized intraperitoneally with 100 μL PBS. Mice were cheek-bled on Day 0, 7, 14, 21, and 28, and serum was isolated for antibody titers. For safety studies, mice were cheek-bled on Day −1, 3, and 21 using EDTA vacutainers (BD, 365974). White blood counts (WBCs) were assessed by automated hemogram by the Animal Care Program Diagnostic Lab. Weights were monitored on Day −1, 3, 7, 10, 14, 17, 21, and 28. Cyclophosphamide mice received 50 mg/kg cyclophosphamide (Sigma, 239785) IP on days 0, 1, and 2 with WBC assessment on day 7 via automated hemogram analysis. For the sepsis model, mice were infected intraperitoneally with 10^7 CFUs *A. baumannii* Lac-4 and monitored twice daily for 7 days for survival. For the pneumonia model, mice were anesthetized with 100 mg/kg ketamine (Koetis) and 10 mg/kg xylazine (VetOne), infected intratracheally with 10^8 CFUs *A. baumannii* in 40 μL PBS using an operating otoscope (Welch Allen) and monitored twice daily for 7 days for survival. For bacterial load determination, mice were infected intraperitoneally with 10^7 CFUs *A. baumannii* Lac-4, humanely euthanized with CO_2 according to IACUC approved protocols, and the spleen, top left lobe of the liver, and kidneys were harvested for enumeration 4 h post-infection as described above. Blood was isolated by cardiac puncture and mixed with sodium heparin for enumeration, or into serum separator tubes for cytokines and antibody titers. The peritoneum was lavaged with 10 mL sterile, ice-cold PBS. Lavage fluid was spun down for 15 minutes at 4000 RPM. The pellet was resuspended in sterile PBS, serially diluted and plated on TSB for enumeration.

Dendritic Cell Activation and Vaccination.

6-week-old female C56BL/6 mice were briefly anesthetized with isoflurane and immunized subcutaneously in the flank with 100 ng Ab-OMVs or Ab-NP. Mock mice were immunized with PBS. Mice were humanely euthanized 24 hours post vaccination and the inguinal lymph nodes were processed for single-cell isolation and stained for the antigen presenting markers CD19 (BD, 557398), CD11c (Invitrogen, 45-0114 82), and F4/80 (eBioscience, 25-4801-82) as well as the activation markers CD40 (BD, 562846), CD80 (BD, 561955), CD86 (BioLegend, 105011), and MHCII (BioLegend, 107652). Cells were also stained with Live/Dead Aqua (Invitrogen, L34957) and Mouse FC Block (BD, 553142). Gates were drawn with single-stained controls and FMOs.

Statistical Analysis and Programs.

Statistical analysis was performed using GraphPad Prism v9. Two-tailed Student's *t*-test was used for comparing two groups. One way analysis of variance (ANOVA) with pairwise comparisons and Tukey post-test correction were used for comparing multiple groups. Matched samples were compared with paired Student's *t*-tests or repeated measures ANOVA. Groups with two or more time points were analyzed using two-way ANOVA with Tukey's multiple comparisons test. Mortality curves were compared using the log-rank (Mantel-Cox) test for significance. Values of $p < 0.05$ were considered statistically significant. Flow cytometry analysis was conducted using FlowJo v10.8.1. Single color compensation was performed for every experiment with more than one fluorophore. Gates were drawn using unstained, single-stained and FMO controls.

Supplementary Material

Refer to Web version on PubMed Central for supplementary material.

ACKNOWLEDGEMENTS

We thank Wangxue Chen (National Research Council, Canada) and Howard Xu (California State University) for providing Ab Lac-4. This work is supported by the National Institute of Health under award number 5T32HL134632-05 (E.B.), the A.P. Giannini Foundation (E.B.), and the Defense Threat Reduction Agency Joint Science and Technology Office for Chemical and Biological Defense under Grant Number HDTRA1-18-1-0014 (L.Z.).

6. REFERENCES

[1]. Antimicrobial Resistance Collaborators, Lancet 2022, DOI 10.1016/S0140-6736(21)02724-0.

[2]. Wallis J, Shenton DP, Carlisle RC, Clin. Exp. Immunol. 2019, 196, 189. [PubMed: 30963549]

[3]. Matić Z, Šantak M, Appl. Microbiol. Biotechnol. 2022, 106, 25. [PubMed: 34889981]

[4]. Rosini R, Nicchi S, Pizza M, Rappuoli R, Front. Immunol. 2020, 11, 1048. [PubMed: 32582169]

[5]. Buchy P, Ascioglu S, Buisson Y, Datta S, Nissen M, Tambyah PA, Vong S, Int. J. Infect. Dis. 2020, 90, 188. [PubMed: 31622674]

[6]. Jansen KU, Anderson AS, Hum. Vaccin. Immunother. 2018, 14, 2142. [PubMed: 29787323]

[7]. Pati R, Shevtsov M, Sonawane A, Front. Immunol. 2018, 9, 2224. [PubMed: 30337923]

[8]. Zhao L, Seth A, Wibowo N, Zhao C-X, Mitter N, Yu C, Middelberg APJ, Vaccine 2014, 32, 327. [PubMed: 24295808]

[9]. Lung P, Yang J, Li Q, Nanoscale 2020, 12, 5746. [PubMed: 32124894]

[10]. Gerritzen MJH, Martens DE, Wijffels RH, van der Pol L, Stork M, Biotechnol. Adv. 2017, 35, 565. [PubMed: 28522212]

[11]. Micoli F, MacLennan CA, Semin. Immunol. 2020, 50, 101433. [PubMed: 33309166]

[12]. van der Pol L, Stork M, van der Ley P, Biotechnol. J. 2015, 10, 1689. [PubMed: 26912077]

[13]. Velimirov B, Ranftler C, Wien. Med. Wochenschr. 2018, 168, 307. [PubMed: 30084090]

[14]. Stanton BA, Genes 2021, 12, DOI 10.3390/genes12071010.

[15]. Yoon H, Ansong C, Adkins JN, Heffron F, Infect. Immun. 2011, 79, 2182. [PubMed: 21464085]

[16]. Jäger J, Keese S, Roessle M, Steinert M, Schromm AB, Cell. Microbiol. 2015, 17, 607. [PubMed: 25363599]

[17]. Dehinwal R, Cooley D, Rakov AV, Alugupalli AS, Harmon J, Cunrath O, Vallabhajosyula P, Bumann D, Schifferli DM, MBio 2021, 12, e0086921. [PubMed: 34061589]

[18]. Balhuizen MD, van Dijk A, Jansen JWA, van de Lest CHA, Veldhuizen EJA, Haagsman HP, mSphere 2021, 6, e0052321. [PubMed: 34232080]

[19]. Kumaraswamy M, Wiull K, Joshi B, Sakoulas G, Kousha A, Vaaje-Kolstad G, Johannessen M, Hegstad K, Nizet V, Askarian F, Microorganisms 2021, 9, DOI 10.3390/microorganisms9102055.

[20]. Elhenawy W, Debelyy MO, Feldman MF, MBio 2014, 5, e00909. [PubMed: 24618254]

[21]. Zhao Z, Wang L, Miao J, Zhang Z, Ruan J, Xu L, Guo H, Zhang M, Qiao W, Sci. Total Environ. 2022, 806, 151403. [PubMed: 34742801]

[22]. Martinez J, Fernandez JS, Liu C, Hoard A, Mendoza A, Nakanouchi J, Rodman N, Courville R, Tuttobene MR, Lopez C, Gonzalez LJ, Shahrestani P, Papp-Wallace KM, Vila AJ, Tolmasky ME, Bonomo RA, Sieira R, Ramirez MS, Sci. Rep. 2019, 9, 17251. [PubMed: 31754169]

[23]. Zhou J, Kroll AV, Holay M, Fang RH, Zhang L, Adv. Mater. 2020, 32, e1901255. [PubMed: 31206841]

[24]. Fang RH, Jiang Y, Fang JC, Zhang L, Biomaterials 2017, 128, 69. [PubMed: 28292726]

[25]. Gorringe AR, Pajón R, Hum. Vaccin. Immunother. 2012, 8, 174. [PubMed: 22426368]

[26]. Schwechheimer C, Kuehn MJ, Nat. Rev. Microbiol. 2015, 13, 605. [PubMed: 26373371]

[27]. Palmieri E, Arato V, Oldrini D, Ricchetti B, Aruta MG, Pansegrau W, Marchi S, Giusti F, Ferlenghi I, Rossi O, Alfini R, Giannelli C, Gasperini G, Necchi F, Micoli F, Vaccines (Basel) 2021, 9, DOI 10.3390/vaccines9030229.

[28]. Centers for Disease Control and Prevention (U.S.), Antibiotic Resistance Threats in the United States, 2019, U.S. Department Of Health And Human Services, Centers For Disease Control And Prevention, 2019.

[29]. Tacconelli E, Carrara E, Savoldi A, Harbarth S, Mendelson M, Monnet DL, Pulcini C, Kahlmeter G, Kluytmans J, Carmeli Y, Ouellette M, Outterson K, Patel J, Cavaleri M, Cox EM, Houchens CR, Grayson ML, Hansen P, Singh N, Theuretzbacher U, Magrini N, WHO Pathogens Priority List Working Group, Lancet Infect. Dis. 2018, 18, 318. [PubMed: 29276051]

[30]. Morris FC, Dexter C, Kostoulias X, Uddin MI, Peleg AY, Front. Microbiol. 2019, 10, 1601. [PubMed: 31379771]

[31]. Mohd Sazlly Lim S, Zainal Abidin A, Liew SM, Roberts JA, Sime FB, J. Infect. 2019, 79, 593. [PubMed: 31580871]

[32]. Ma C, McClean S, Vaccines (Basel) 2021, 9, DOI 10.3390/vaccines9060570.

[33]. Perez S, Innes GK, Walters MS, Mehr J, Arias J, Greeley R, Chew D, MMWR Morb. Mortal. Wkly. Rep. 2020, 69, 1827. [PubMed: 33270611]

[34]. Lai C-C, Wang C-Y, Hsueh P-R, J. Microbiol. Immunol. Infect. 2020, 53, 505. [PubMed: 32482366]

[35]. García-Garmendia JL, Ortiz-Leyba C, Garnacho-Montero J, Jiménez-Jiménez FJ, Pérez-Paredes C, Barrero-Almodóvar AE, Gili-Miner M, Clin. Infect. Dis. 2001, 33, 939. [PubMed: 11528563]

[36]. Gellings PS, Wilkins AA, Morici LA, Pathogens 2020, 9, DOI 10.3390/pathogens9121066.

[37]. Ma C, Chen W, Expert Rev. Vaccines 2021, 20, 281. [PubMed: 33554671]

[38]. Jin JS, Kwon S-O, Moon DC, Gurung M, Lee JH, Kim SI, Lee JC, PLoS One 2011, 6, e17027. [PubMed: 21386968]

[39]. Jun SH, Lee JH, Kim BR, Kim SI, Park TI, Lee JC, Lee YC, PLoS One 2013, 8, e71751. [PubMed: 23977136]

[40]. Kwon S-O, Gho YS, Lee JC, Kim SI, FEMS Microbiol. Lett. 2009, 297, 150. [PubMed: 19548894]

[41]. Fang RH, Kroll AV, Gao W, Zhang L, Adv. Mater. 2018, 30, e1706759. [PubMed: 29582476]

[42]. Gao W, Fang RH, Thamphiwatana S, Luk BT, Li J, Angsantikul P, Zhang Q, Hu C-MJ, Zhang L, Nano Lett. 2015, 15, 1403. [PubMed: 25615236]

[43]. Reddy ST, van der Vlies AJ, Simeoni E, Angeli V, Randolph GJ, O'Neil CP, Lee LK, Swartz MA, Hubbell JA, Nat. Biotechnol. 2007, 25, 1159. [PubMed: 17873867]

[44]. Valentine SC, Contreras D, Tan S, Real LJ, Chu S, Xu HH, J. Clin. Microbiol. 2008, 46, 2499. [PubMed: 18524965]

[45]. Zhou J, Karshalev E, Mundaca-Uribe R, Esteban-Fernández de Ávila B, Krishnan N, Xiao C, Ventura CJ, Gong H, Zhang Q, Gao W, Fang RH, Wang J, Zhang L, Adv. Mater. 2021, e2103505. [PubMed: 34599770]

[46]. Gao W, Hu C-MJ, Fang RH, Luk BT, Su J, Zhang L, Adv. Mater. 2013, 25, 3549. [PubMed: 23712782]

[47]. Arvizo R, Bhattacharya R, Mukherjee P, Expert Opin. Drug Deliv. 2010, 7, 753. [PubMed: 20408736]

[48]. Alkilany AM, Murphy CJ, J. Nanopart. Res. 2010, 12, 2313. [PubMed: 21170131]

[49]. He C, Hu Y, Yin L, Tang C, Yin C, Biomaterials 2010, 31, 3657. [PubMed: 20138662]

[50]. Harris G, KuoLee R, Xu HH, Chen W, Sci. Rep. 2019, 9, 6538. [PubMed: 31024025]

[51]. George E, Goswami A, Lodhiya T, Padwal P, Iyer S, Gauttam I, Sethi L, Jeyasankar S, Sharma PR, Dravid AA, Mukherjee R, Agarwal R, bioRxiv 2022, 2022.06.07.495204.

[52]. Wu G, Ji H, Guo X, Li Y, Ren T, Dong H, Liu J, Liu Y, Shi X, He B, Nanomedicine 2020, 24, 102148. [PubMed: 31887427]

[53]. Feng C, Li Y, Ferdows BE, Patel DN, Ouyang J, Tang Z, Kong N, Chen E, Tao W, Acta Pharm Sin B 2022, 12, 2206. [PubMed: 35013704]

[54]. Momose H, Mizukami T, Ochiai M, Hamaguchi I, Yamaguchi K, J. Biomed. Biotechnol. 2010, 2010, 361841. [PubMed: 20617152]

[55]. Oli AN, Oli UC, Ejiofor OS, Nwoye CU, Esimone CO, Trials in Vaccinology 2016, 5, 8.

[56]. Breslow JM, Meissler JJ Jr, Hartzell RR, Spence PB, Truant A, Gaughan J, Eisenstein TK, Infect. Immun. 2011, 79, 3317. [PubMed: 21576323]

[57]. van Faassen H, KuoLee R, Harris G, Zhao X, Conlan JW, Chen W, Infect. Immun. 2007, 75, 5597. [PubMed: 17908807]

[58]. Koprnová J, Svetlanský I, Babel'a R, Bilíková E, Hanzen J, Zuscáková IJ, Mílovský V, Masár O, Kovacicová G, Gogová M, Koren P, Rusnák M, Lisková A, Zák V, Karvaj M, Kanik K, Strehár A, Lesay M, Szöveniová Z, Trupl J, Purgelová A, Kralinský K, Roidová A, Lamosová J, Huttová M, Krcméry V, Scand. J. Infect. Dis. 2001, 33, 891. [PubMed: 11868760]

[59]. Gu Y, Jiang Y, Zhang W, Yu Y, He X, Tao J, Hou X, Wang H, Deng M, Zhou M, Xu J, Diagn. Microbiol. Infect. Dis. 2021, 99, 115229. [PubMed: 33161239]

[60]. Jacobs AC, Thompson MG, Black CC, Kessler JL, Clark LP, McQueary CN, Gancz HY, Corey BW, Moon JK, Si Y, Owen MT, Hallock JD, Kwak YI, Summers A, Li CZ, Rasko DA, Penwell WF, Honnold CL, Wise MC, Waterman PE, Lesho EP, Stewart RL, Actis LA, Palys TJ, Craft DW, Zurawski DV, MBio 2014, 5, e01076. [PubMed: 24865555]

[61]. Inchai J, Pothirat C, Bumroongkit C, Limsukon A, Khositsakulchai W, Liwsrisakun C, Intensive Care Med J 2015, 3, 9.

[62]. Li YJ, Pan CZ, Fang CQ, Zhao ZX, Chen HL, Guo PH, Zhao ZW, BMC Infect. Dis. 2017, 17, 371. [PubMed: 28558660]

[63]. Čiginskienė A, Dambrauskienė A, Rello J, Adukauskienė D, Medicina 2019, 55, 49. [PubMed: 30781896]

[64]. Hamidian M, Nigro SJ, Microb. Genom. 2019, 5, DOI 10.1099/mgen.0.000306.

[65]. Jan AT, Front. Microbiol. 2017, 8, 1053. [PubMed: 28649237]

[66]. Xiang SD, Scholzen A, Minigo G, David C, Apostolopoulos V, Mottram PL, Plebanski M, Methods 2006, 40, 1. [PubMed: 16997708]

[67]. Fifis T, Gamvrellis A, Crimeen-Irwin B, Pietersz GA, Li J, Mottram PL, McKenzie IFC, Plebanski M, Immunol J 2004, 173, 3148.

[68]. Hu X, Zhang Y, Ding T, Liu J, Zhao H, Front Bioeng Biotechnol 2020, 8, 990. [PubMed: 32903562]

[69]. Rossi O, Citiulo F, Mancini F, Hum. Vaccin. Immunother. 2021, 17, 601. [PubMed: 32687736]

[70]. Warren HS, Fitting C, Hoff E, Adib-Conquy M, Beasley-Topliffe L, Tesini B, Liang X, Valentine C, Hellman J, Hayden D, Cavaillon J-M, J. Infect. Dis. 2010, 201, 223. [PubMed: 20001600]

[71]. Steeghs L, den Hartog R, den Boer A, Zomer B, Roholl P, van der Ley P, Nature 1998, 392, 449. [PubMed: 9548250]

[72]. Peng D, Hong W, Choudhury BP, Carlson RW, Gu X-X, Infection and Immunity 2005, 73, 7569. [PubMed: 16239560]

[73]. Boll JM, Crofts AA, Peters K, Cattoir V, Vollmer W, Davies BW, Stephen Trent M, Proceedings of the National Academy of Sciences 2016, 113, E6228.

[74]. Moffatt JH, Harper M, Mansell A, Crane B, Fitzsimons TC, Nation RL, Li J, Adler B, Boyce JD, Infection and Immunity 2013, 81, 684. [PubMed: 23250952]

[75]. Pulido MR, García-Quintanilla M, Pachón J, McConnell MJ, Vaccine 2020, 38, 719. [PubMed: 31843268]

[76]. Harris G, Kuo Lee R, Lam CK, Kanzaki G, Patel GB, Xu HH, Chen W, Antimicrob. Agents Chemother. 2013, 57, 3601. [PubMed: 23689726]

[77]. Luo G, Lin L, Ibrahim AS, Baquir B, Pantapalangkoor P, Bonomo RA, Doi Y, Adams MD, Russo TA, Spellberg B, PLoS One 2012, 7, e29446. [PubMed: 22253723]

[78]. Kanekiyo M, Joyce MG, Gillespie RA, Gallagher JR, Andrews SF, Yassine HM, Wheatley AK, Fisher BE, Ambrozak DR, Creanga A, Leung K, Yang ES, Boyoglu-Barnum S, Georgiev IS, Tsybovsky Y, Prabhakaran MS, Andersen H, Kong W-P, Baxa U, Zephir KL, Ledgerwood JE, Koup RA, Kwong PD, Harris AK, McDermott AB, Mascola JR, Graham BS, Nat. Immunol. 2019, 20, 362. [PubMed: 30742080]

[79]. Gao NJ, Uchiyama S, Pill L, Dahesh S, Olson J, Bautista L, Maroju S, Berges A, Liu JZ, Zurich RH, van Sorge NM, Fairman J, Kapoor N, Nizet V, Infectious Microbes & Diseases 2021, 3, 87.

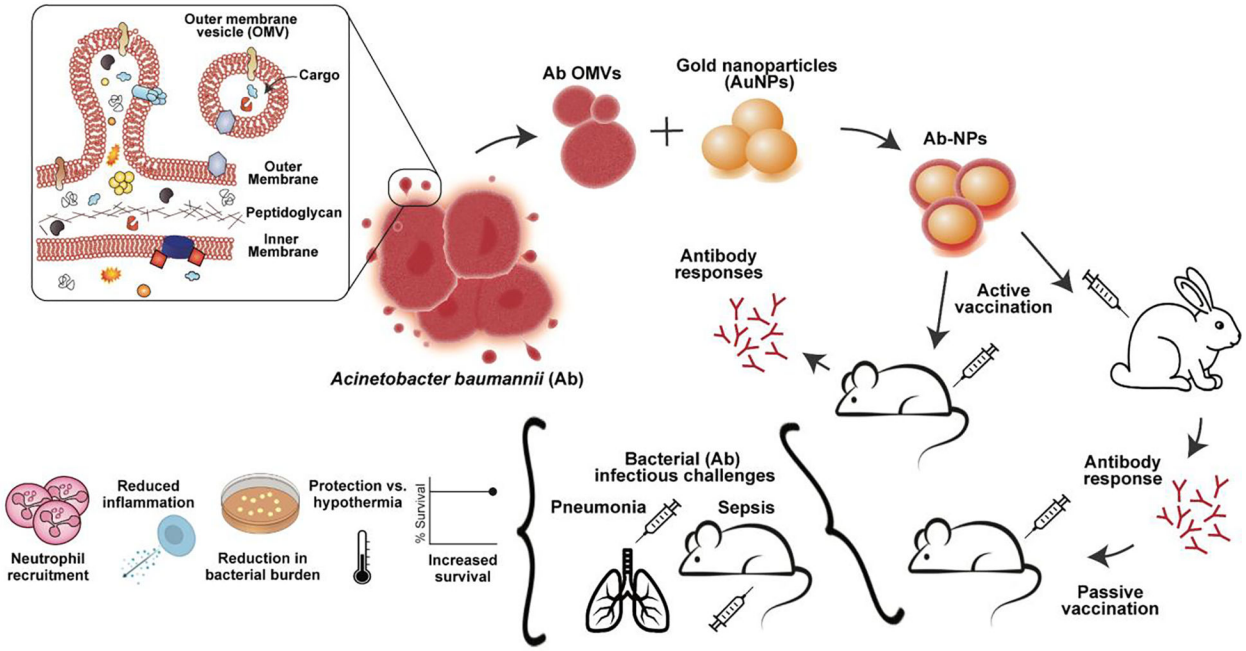

Figure 1. ***Acinetobacter baumannii*** **OMV-derived nanoparticle vaccine.**

Outer membrane vesicles (OMVs) were isolated from the hypervirulent *A. baumannii* clinical isolate Lac-4 and associated with inert gold nanoparticle cores (AuNPs) to generate an *A. baumannii* nanoparticle vaccine (Ab-NP). Vaccination with Ab-NPs evoked *A. baumannii* specific immunity in mice and rabbits. Passive vaccination with immune rabbit serum protected mice against bacterial challenge in a lethal sepsis model. Active vaccination with Ab-NPs protected mice against bacterial challenge in lethal pneumonia and sepsis models. Vaccination induced neutrophil recruitment, reduced systemic inflammation, protected mice from sepsis-induced hypothermia, and controlled bacterial burdens.

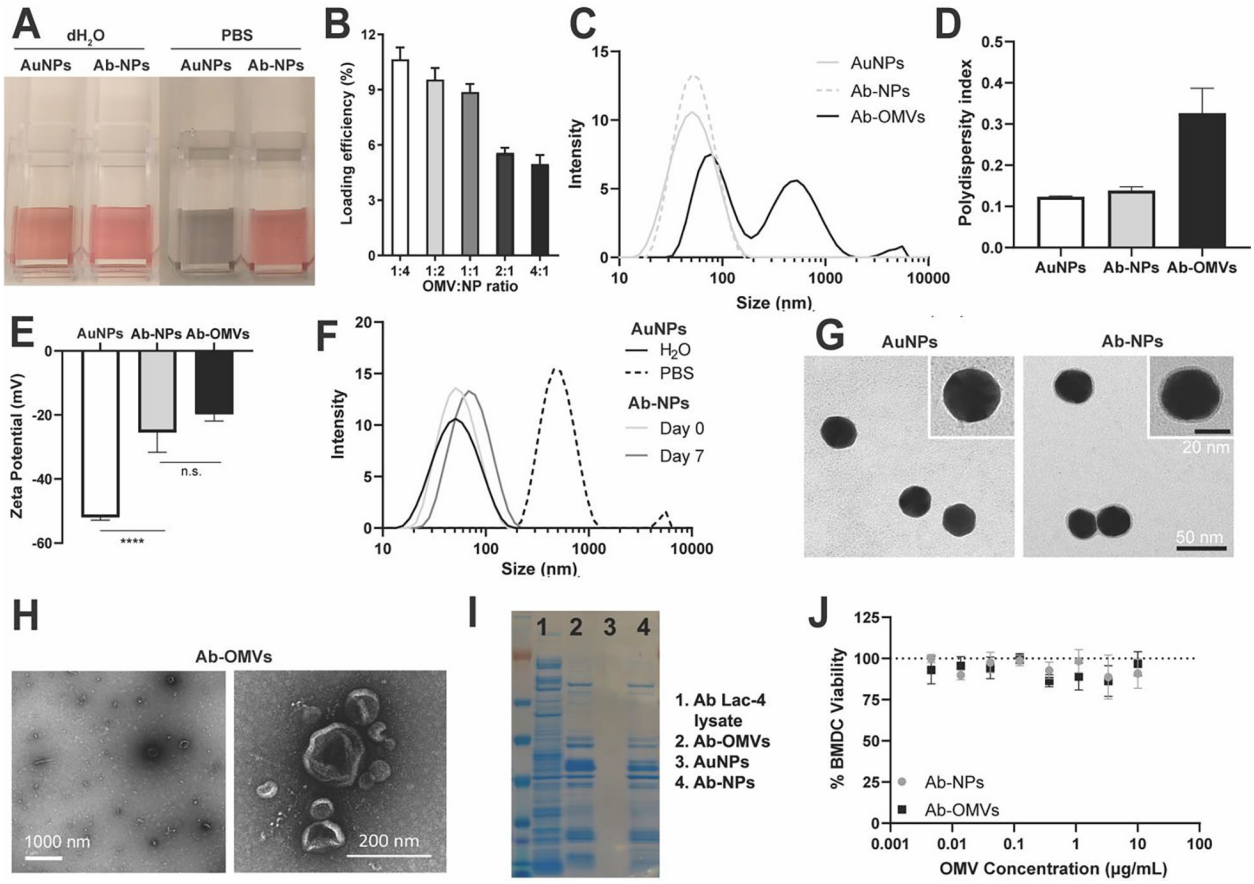

Figure 2. Characterization of Ab-NPs.

(A) A representative image showing the stability of AuNPs and Ab-NPs in dH_2O or PBS. Mean of technical replicates ± SD. **(B)** Quantification of Ab-OMV loading efficiency with optimal efficiency reached at a 1:1 ratio of Ab-OMVs to NPs. **(C)** Hydrodynamic sizes (diameter, nm) of AuNPs, Ab-NPs, and Ab-OMVs. **(D)** Polydispersity indices of AuNPs, Ab-NPs, and Ab-OMVs. Mean of technical replicates ± SD. **(E)** Surface zeta potentials (mV) of AuNPs, Ab-NPs and Ab-OMVS. Mean of technical replicates ± SD. **** $p < 0.0001$ **(F)** Stability of AuNPs as measured by hydrodynamic size (diameter, nm) of AuNPs in dH_2O or PBS and Ab-NPs in PBS on day 0 and day 7. **(G)** Representative TEM images showing the AuNP cores and Ab-NPs. Inset: a zoomed-in view of a single AuNP or Ab-NP nanoparticle. Scale bar 50 nm (main) and 20 nm (inset). **(H)** Representative TEM images showing Ab-OMVs. Scale bar 1000 nm (left image) and 200 nm (right image). **(I)** Protein loading of Ab-NPs compared to Ab Lac-4 whole cell lysate, AuNPs and Ab-OMVs. Proteins were stained with Coomassie Blue. **(J)** BMDC viability as measured by PrestoBlue when incubated with increasing OMV concentrations of Ab-NPs or Ab-OMVs. Mean of technical replicates ± SD. A-J representative of 2–3 independent experiments.

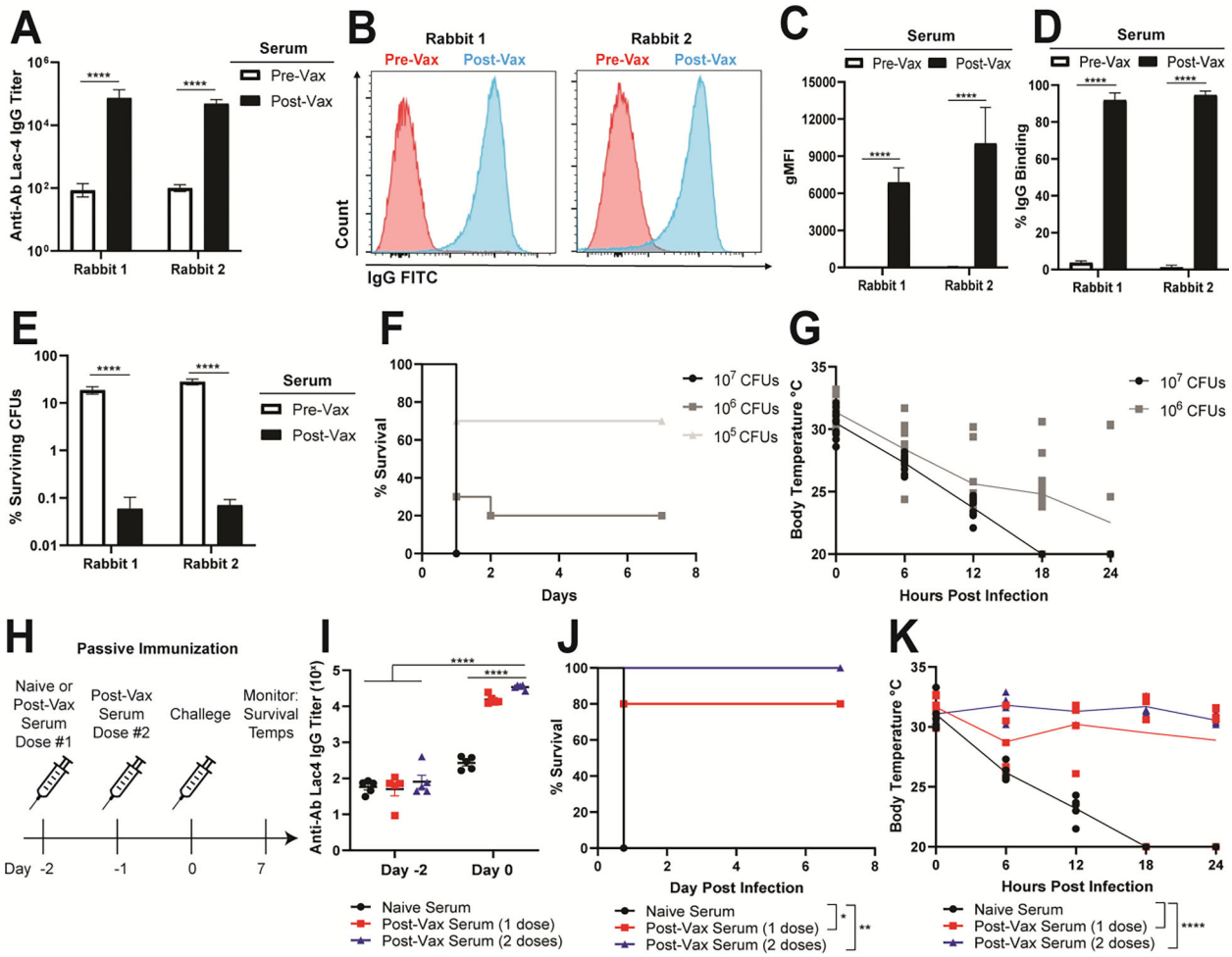

Figure 3. Ab-NP post-vax serum binds Ab and is protective during passive immunization.

(A) IgG antibody titers specific for Ab Lac-4 from pre-vax and post-vax serum obtained from two New Zealand white rabbits (AbNova). Pooled means of technical replicates from three independent experiments ± SEM. **** $p < 0.0001$ **(B)** Histograms of rabbit IgG from pre-vax (blue) and post-vax (red) serum bound to live Ab Lac-4 measured by flow cytometry. Images are representative of technical replicates from three independent experiments. **(C)** Fold binding of rabbit IgG from pre-vax and post-vax serum bound to live Ab Lac-4 measured by flow cytometry. Pre-vax binding was normalized to 1.0. Pooled means of technical replicates from three independent experiments ± SEM. * $p < 0.05$, **** $p < 0.0001$. **(D)** Geometric mean fluorescence intensity (gMFI) of rabbit IgG from pre-vax and post-vax serum bound to live Ab Lac-4 measured by flow cytometry. Pooled means of technical replicates from three independent experiments ± SEM. *** $p < 0.001$ **** $p < 0.0001$. **(E)** Opsonophagocytic killing of Ab Lac-4 by healthy human neutrophils incubated with pre-vax or post-vax rabbit serum. Percent surviving colony forming units (CFUs) relative to starting inputs is graphed. Pooled means of technical replicates from three independent experiments ± SEM. **** $p < 0.0001$. **(F)** Mortality curves in mice infected with Ab Lac-4 intraperitoneally (IP) with 10^7, 10^6, or 10^5 CFUs in sterile PBS. Mice were monitored for survival for 7 d. Two independent experiments were pooled for

each infectious dose (n=10 per group). **(G)** Core body temperatures in mice infected with Ab Lac-4 IP with 10^7 or 10^6 CFUs. Surface temperatures were measured using an infrared thermometer gun at the base of the tail at the time of infection and every 6 h for 24 h. Two independent experiments were pooled for each infectious dose with each dot representing an individual mouse (n=10 per group). **(H)** Passive immunization scheme using naïve (Sigma) or post-vax rabbit serum. Mice were given naïve serum or post-vax serum intravenously through retro-orbital injection 2 d before infection. One group of mice received a second dose of post-vax serum 24 h later. Antibody titers were assessed on Day −2 and Day 0 by submandibular blood collection and ELISA. All mice were infected IP with 10^7 CFUs and monitored for survival and body temperature. **(I)** IgG antibody titers specific for Ab Lac-4 from mice Day −2 and Day 0. Each dot represents one mouse. Representative of two independent experiments. **** $p < 0.0001$ **(J)** Mortality curves in mice infected with 10^7 CFUs Ab Lac-4 IP. Mice were monitored for survival for 7 days. Representative of two independent experiments (n=5 per group). **(K)** Core body temperatures in mice infected with 10^7 CFUs Ab Lac-4 IP. Temperatures were measured using an infrared thermometer gun at the base of the tail at the time of infection and every 6 h for 24 h. Each dot represents one mouse. Representative of two independent experiments (n=5 per group).

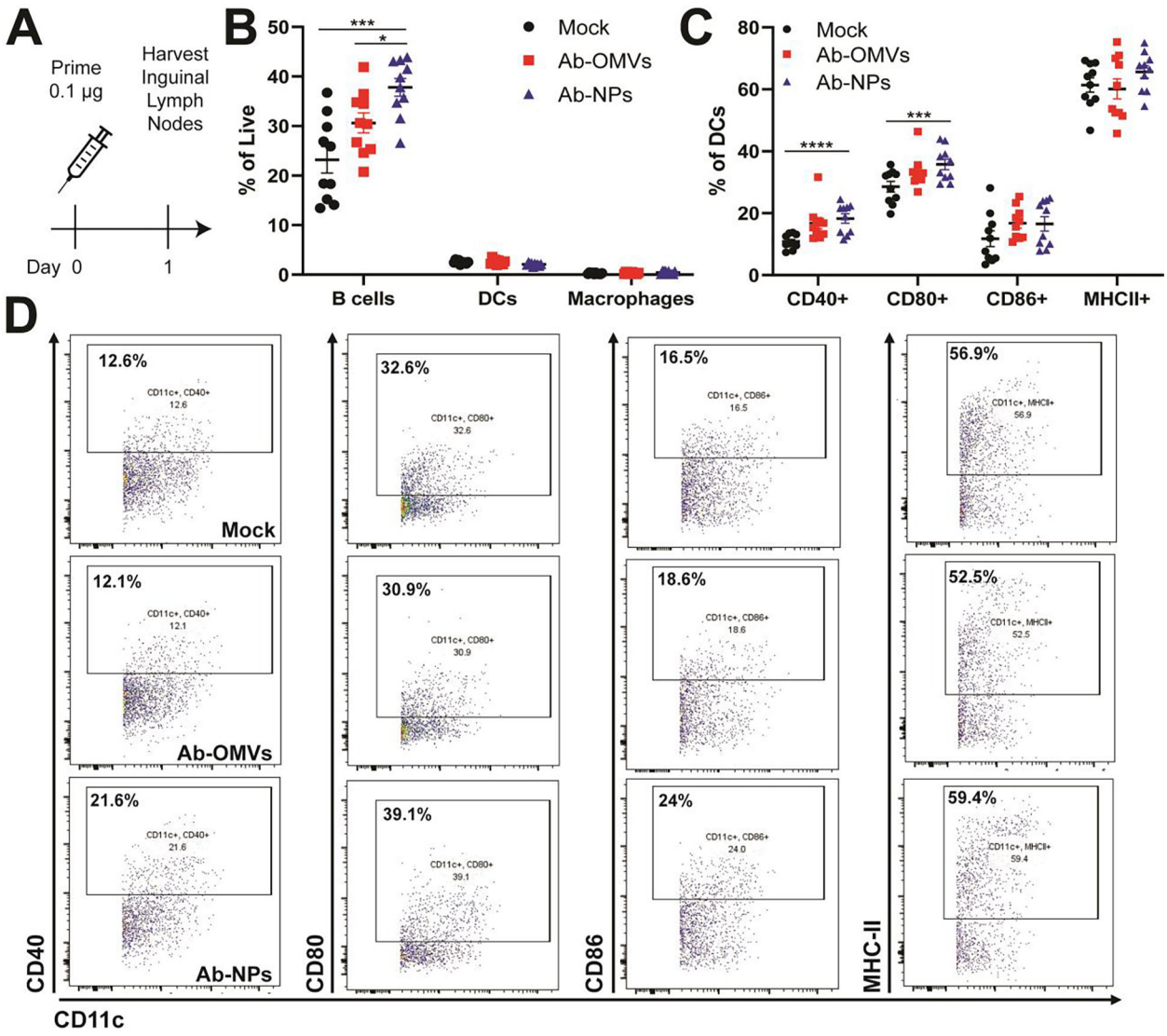

Figure 4. Ab-NPs induce antigen presenting cells in draining lymph nodes.

(A) Mice were vaccinated with PBS (Mock), 100 ng Ab-OMVs or 100 ng Ab-NPs. 24 h later, inguinal lymph nodes (ILN) were harvested, processed for single-cell isolation, and stained for analysis by flow cytometry. Gates were drawn using single stained controls and FMOs. Dendritic cells were gated on cells, singlets, Live, F4/80^{-}CD11c^{+} and then further individually gated for activation markers CD40, CD80, CD86, and MHC-II. B cells were gated cells, singlets, Live, CD19^{+}. Macrophages were gated cells, singlets, live, F4/80^{+}CD11c^{-}. **(B)** Representative flow plots and **(C)** quantification of the activation markers CD40, CD80, CD86, and MHC-II expressed by CD11c^{+} dendritic cells in inguinal lymph nodes 24 hours post vaccination. **(A)** Representative of two independent experiments (n=10), **(B)** Two independent experiments were pooled with each dot representing a single mouse (n=10). **(D)** Quantification of percent of B cells, dendritic cells (DCs) and F4/80+ macrophages of total live cells in the ILN. Two independent experiments were pooled with each dot representing a single mouse (n=10).

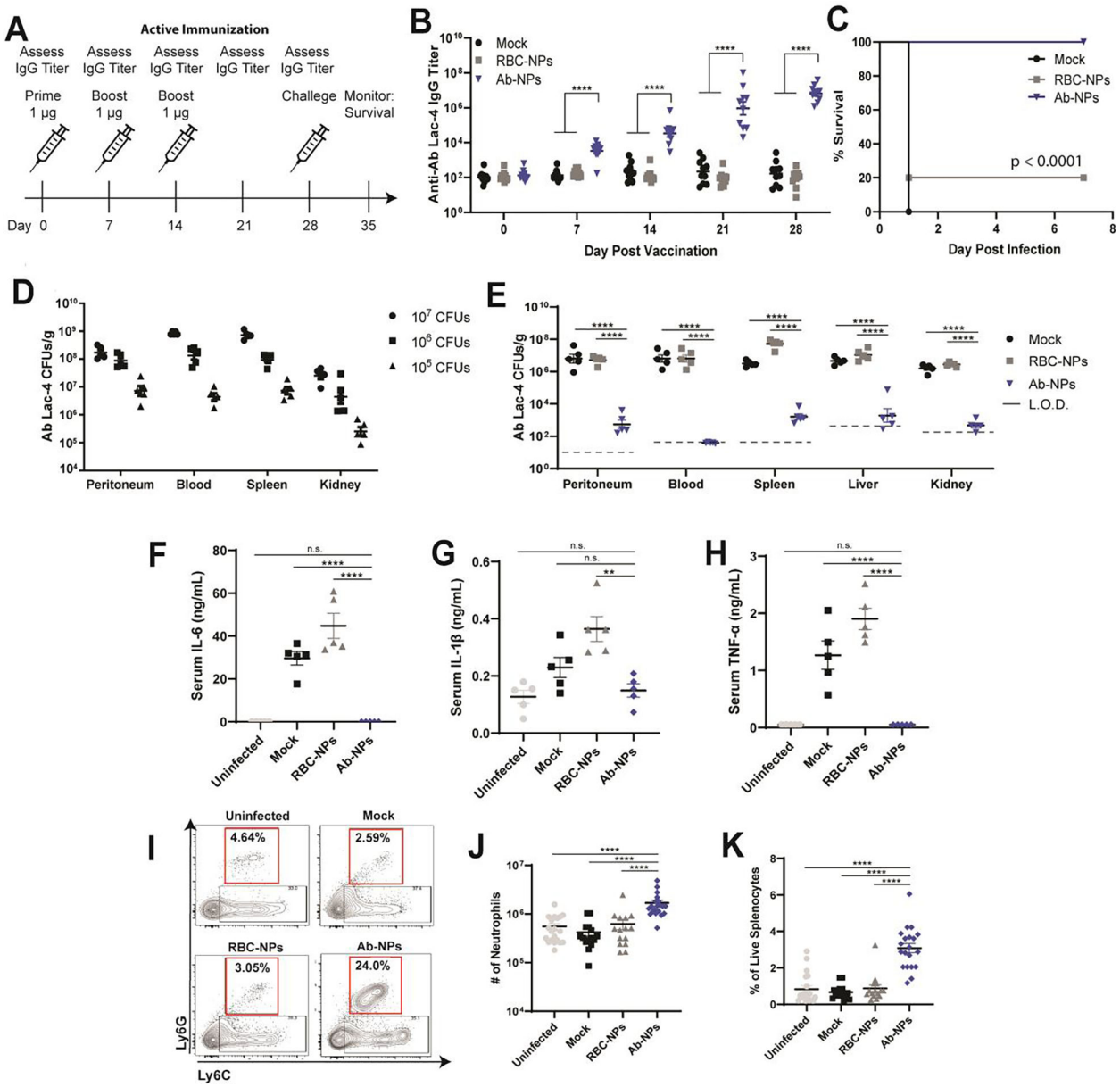

Figure 5. Ab-NP vaccination protects mice from lethal sepsis.

(A) Active immunization scheme with PBS (mock), red blood cell NPs (RBC-NPs), or Ab-NPs. Mice were immunized IP with 1 μg antigen in 100 μL sterile PBS on days 0, 7, and 14. Ab Lac-4 IgG titers were assessed weekly prior to immunization by submandibular blood collection and ELISA. Mice were challenged on Day 28 and monitored for survival for seven days. **(B)** IgG antibody titers specific for Ab Lac-4 from mice pre-vaccination and post vaccination prior to challenge. Each dot represents one mouse. Representative of 3 (RBC-NP) or 4 (Mock, Ab-NPs) independent experiments (n=10 per group) **** $p < 0.0001$ **(C)** Mortality curves in immunized mice infected with 10^7 CFUs Ab Lac-4 IP. Mice were monitored for survival for seven days. Pooled survival from two independent experiments per group (n=10). **(D)** Organ CFUs from mice infected with 10^7, 10^6, or 10^5 CFUs Ab Lac-4 IP in sterile PBS. CFUs were assessed 4 hours post infection. Each dot

represents one mouse. Representative of two independent experiments (n=5 per group). **(E)** Organ CFUs from mice infected with 10^7 CFUs Ab Lac-4 IP. CFUs were assessed 4 hours post infection. Each dot represents one mouse. Representative of 2 (RBC-NP) or 3 (PBS, Ab-NPs) independent experiments. **** $p < 0.0001$. **(F-H)** Serum cytokines from vaccinated mice infected with 10^7 CFUs Ab Lac-4 IP. Blood was collected by cardiac puncture 4 h after infection and serum was isolated. Each dot represents one mouse. Representative of 2 (RBC-NP) or 3 (PBS, Ab-NPs) independent experiments (n=5 per group). * $p < 0.05$, ** $p < 0.01$, **** $p < 0.0001$. **(I)** Representative flow plots and J & K) quantification of splenic neutrophils from vaccinated mice infected with 10^7 CFUs Ab Lac-4 IP. Spleens were harvested 4 hours post infection, processed for single-cell isolation, and stained for analysis by flow cytometry. Gating: Cells, singlets, Live, $CD11b^+$, $Ly6G^{hi}Ly6C^{int}$. Gates were drawn using single stained controls and fluorescence minus ones (FMOs). **(J and K)** 3–4 independent experiments were pooled, n=15–20 per group; n.s. not significant. **** $p < 0.0001$.

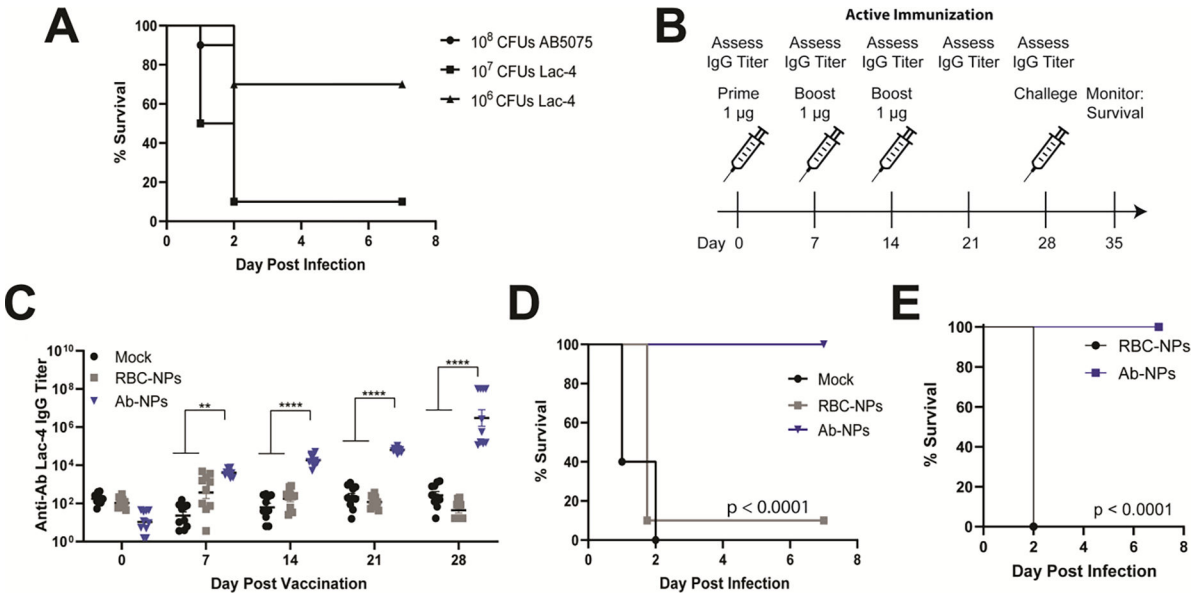

Figure 6. Ab-NP vaccination protects against lethal pneumonia.

(A) Mortality curves in mice infected with 10^8 CFUs AB5075, 10^7 or 10^6 CFUs Ab Lac-4 intratracheally (IT) in sterile PBS. Mice were anesthetized with 100 mg/kg ketamine and 10 mg/kg xylazine prior to infection. Two independent experiments were pooled for each infectious dose (n=10 per group). **(B)** Active immunization scheme with PBS (mock), red blood cell NPs (RBC-NPs, nanoparticle control) or Ab-NP. Mice were immunized IP with 1 µg antigen in 100 µL sterile PBS on days 0, 7, and 14. Ab Lac-4 IgG titers were assessed weekly prior to immunization by submandibular blood collection and ELISA. Mice were challenged on Day 28 and monitored for survival for seven days. **(C)** IgG antibody titers specific for Ab Lac-4 from mice pre-vaccination and post vaccination prior to challenge. Each dot represents one mouse. Representative of 2 independent experiments (n=10 per group) **** $p < 0.0001$. **(D)** Mortality curves in immunized mice infected with 10^8 CFUs Ab Lac-4 IP. Mice were monitored for survival for seven days. Pooled survival from two independent experiments per group (n=10). **(E)** Mortality curves in immunized mice infected with 10^7 CFUs Ab Lac-4 IP 30 weeks post vaccination. Mice were monitored for survival for seven days. Pooled survival from two independent experiments per group (n=10).